

# Petrologic Evolution of Anorthoclase Phonolite Lavas at Mount Erebus, Ross Island, Antarctica

by P. R. KYLE<sup>1</sup>, J. A. MOORE<sup>1</sup>, AND M. F. THIRLWALL<sup>2</sup>

<sup>1</sup>*Department of Geoscience, New Mexico Institute of Mining and Technology, Socorro, New Mexico 87801*

<sup>2</sup>*Department of Geology, Royal Holloway and Bedford New College, Egham TW20 0EX, UK*

(Received 2 November 1988; revised typescript accepted 18 October 1991)

## ABSTRACT

Mount Erebus, Ross Island, Antarctica, is an active, intraplate, alkaline volcano. The strongly undersaturated sodic lavas range from basanite to anorthoclase phonolite, and are termed the Erebus lineage (EL). The lavas are porphyritic with olivine ( $\text{Fo}_{88-51}$ ), clinopyroxene ( $\text{Wo}_{45-53}\text{En}_{36-41}\text{Fs}_{8-30}$ ), opaque oxides ( $\text{Usp}_{51-76}$ ), feldspar ( $\text{An}_{72-11}$ ), and apatite. Rare earth element (REE) contents increase only slightly with increasing differentiation compared with other incompatible elements. The light REE are enriched ( $\text{La}_N/\text{Yb}_N = 14-20$ ) and there are no significant Eu anomalies.  $^{87}\text{Sr}/^{86}\text{Sr}$  is uniform and low ( $\sim 0.7030$ ) throughout the EL, suggesting derivation of the basanites from a depleted asthenospheric mantle source, and lack of significant crustal contamination during fractionation of the basanite. Regular geochemical trends indicate that the EL evolved from the basanites by fractional crystallization. Major element mass balance calculations and trace element models show that fractionation of 16% olivine, 52% clinopyroxene, 14% Fe-Ti oxides, 11% feldspar, 3% nepheline, and 3% apatite from a basanite parent leaves 23.5% anorthoclase phonolite.

Minor volumes of less undersaturated, more iron-rich benmoreite, phonolite, and trachyte are termed the enriched iron series (EFS). The trachytes have  $^{87}\text{Sr}/^{86}\text{Sr}$  of 0.704, higher than other EFS and EL rocks, and they probably evolved by a combined assimilation-fractional crystallization process.

The large volume of phonolite at Mt. Erebus requires significant basanite production. This occurs by low degrees of partial melting in a mantle plume (here termed the Erebus plume) rising at a rate of about 6 cm/yr.

## INTRODUCTION

The McMurdo Volcanic Group (MVG) (Kyle & Cole, 1974; Kyle, 1990a) consists of Late Cenozoic intraplate alkaline volcanics erupted through rifted continental crust on the western margin of the Ross Embayment, Antarctica. MVG rocks in the McMurdo Sound area comprise the Erebus volcanic province and range from basanite to phonolite and trachyte (Kyle, 1990b). Ross Island comprises Mt. Erebus, an active, 3974 m high composite volcano, surrounded radially by smaller volcanic centers at Mt. Terror, Mt. Bird, and Hut Point Peninsula, dating back to 5 Ma (Armstrong, 1978).

Two distinct volcanic lineages occur on Ross Island. Lavas at the centers surrounding Mt. Erebus consist mainly of basanite with minor microporphyritic, kaersutite-bearing intermediate differentiates and phonolite. These were examined in detail by Kyle (1981a, 1981b) in Dry Valley Drilling Project (DVDP) cores from Hut Point Peninsula and were termed the DVDP lineage. In contrast, Mt. Erebus consists predominantly of anorthoclase-phyric phonolite with minor amounts of basanite and strongly porphyritic intermediate lavas. Kaersutite does not occur in these lavas, which are termed the Erebus lineage (EL) (Kyle, 1976). Very minor volumes of distinctly less undersaturated and microporphyritic lavas also occur on Mt. Erebus and are termed the enriched iron (Fe) series (EFS).

Here we examine the mineralogy, geochemistry, and petrogenesis of lavas from Mt. Erebus and compare them with the evolution of the DVDP lineage. Recent volcanic ejecta from Mt. Erebus (Kyle, 1977) are generally similar to the older anorthoclase phonolite lavas, and are not discussed.

### VOLCANIC GEOLOGY

The volcanic geology of Mt. Erebus has been described by Moore & Kyle (1987). Lava flows, dikes, and pyroclastic deposits of intermediate composition and lesser basanite are exposed in eroded cones which form sea cliffs and small offshore islands on the southwest side of Mt. Erebus, and in Fang Ridge on the northeast flank. Outcrops on the gently inclined lower slopes of Mt. Erebus are mostly anorthoclase phonolite. The steep upper slopes of Mt. Erebus consist of short, thick glassy anorthoclase phonolite flows. The summit region is a gently sloping plateau infilling a caldera, which has a rim at  $\sim 3200$  m. A persistent convecting anorthoclase phonolite lava lake occupies a pit crater within a composite cone on the south side of this plateau (Kyle *et al.*, 1982). Benmoreite, phonolite, and trachyte of the EFS occur as endogenous domes at Mt. Cis, Lewis Bay, Aurora Glacier, and Bomb Peak, and as flows interbedded with EL lavas in the Dellbridge Islands.

Although exposures are limited on Mt. Erebus and there is no deep erosion, apart from Fang Ridge, we believe that anorthoclase phonolite is the dominant rock type, possibly exceeding 75% by volume. EFS lavas constitute  $\ll 1\%$ .

### PETROGRAPHY

The lava nomenclature follows Coombs & Wilkinson (1969) and has been described, along with detailed petrographic descriptions, by Moore & Kyle (1987). This nomenclature allows easy comparison with published work on the DVDP lineage (Kyle, 1981*b*). In the

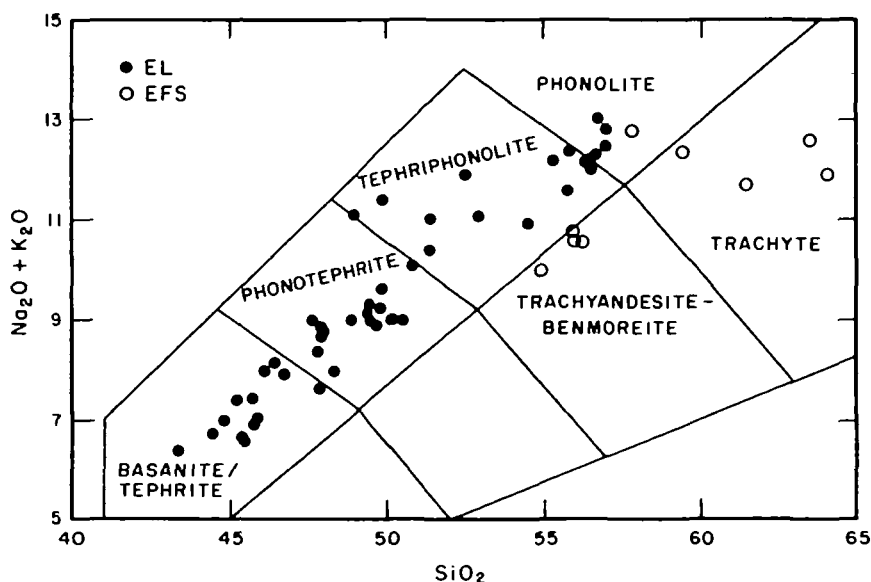


FIG. 1. Classification of Mt. Erebus rocks using the total alkalis-silica diagram (Le Bas *et al.*, 1986). (Note the lower alkalis in the EFS rocks compared with EL rocks.)

TABLE 1  
 Generalized petrographic summary of Mt. Erebus volcanic rocks

Rock type	Texture	Mineralogy							Groundmass
		Ol	Cpx	Kaer	Op	Fsp	Ap	Fsph	
Basanite	fp(10-25)	p, x	p		p	p	p	g	p, i
Ne hawaiiite	fp(1-20) or cp(20-50)	p, po	r-p, po	r, po, x?	p	p	p	r-g	i, p or gl-h 2c, 2o
Ne mugearite	cp(20-30)	p, po	p, po		p	p	p	g	i, p, 2o
Ne benmoreite	cp(20-50)	p, po, x	r-p		p	p	p	g	i, p or gl
Anorthoclase phonolite	cp(30-60)	p	p		p	p	p	r-g	i, p or gl-h, c
Benmoreite	mp(10-20)	p, po, x	r-p	r-p, po	p	p-x	r		t or gl, c
Phonolite	mp(3-10) or p(10-15)	r-p, x	r-g	r-p po-co	r-p	p, x	r	g	t or h-i, p
Trachyte	mp(<5)	g-x	p		p	p			t

*Abbreviations:*

Texture: p—porphyritic; mp—microporphyritic; fp—finely porphyritic; cp—coarsely porphyritic; percentage of phenocrysts to nearest 5% is given in parentheses.

Mineralogy: Ol—olivine; Cpx—clinopyroxene; Kaer—kaersutite; Op—opaque oxides; Fsp—feldspar; Ap—apatite; Fspth—feldspathoids; p—present (> 1%); r—rare (< 1%); x—xenocrystic; po—partially oxidized; co—completely oxidized; g—groundmass only.

Groundmass: i—intersertal; p—pilotaxitic; gl—glassy; h—hyalophitic; c—cryptocrystalline; t—trachytic; 2c—secondary carbonate; 2o—secondary oxidation.

total alkali-silica classification (Le Bas *et al.*, 1986), EL rocks are tephrite/basanite, phonotephrite, tephriphonolite, and phonolite (Fig. 1). EFS rocks are benmoreite, trachyte, and one is a phonolite. General petrographic features are summarized in Table 1. All EL lavas are coarsely porphyritic (phenocrysts up to 5 cm), except the basanites and some Ne hawaiites, which are finely porphyritic (phenocrysts up to 5 mm). A similar phenocryst assemblage of olivine, clinopyroxene, opaque oxides, feldspar, apatite, and accessory pyrrhotite and feldspathoids occurs throughout the lineage. The groundmasses are pilotaxitic and intersertal to glassy, and groundmass phases are similar to phenocrysts. EFS lavas are generally trachytic textured with scarce microphenocrysts of olivine, clinopyroxene, kaersutite, opaque oxides, and both alkali and plagioclase feldspar.

### MINERAL CHEMISTRY

Mineral phases were analyzed by ARL-EMX electron microprobe using 15 kV accelerating potential,  $(2-3) \times 10^{-8}$  A sample current, 1-2  $\mu\text{m}$  beam, natural mineral standards, and the correction factors of Bence & Albee (1968).

#### *Olivine*

Olivine is ubiquitous in EL lavas as 1-5 mm euhedral and subhedral phenocrysts, and varies continuously from  $\text{Fo}_{88}$  in basanite to  $\text{Fo}_{51}$  in anorthoclase phonolite (Fig. 2). Xenocrysts occur rarely in the basanites, and in Ne benmoreite (sample 25748) xenocrysts of  $\text{Fo}_{73-71}$  are probably derived from a basanite. In EFS lavas olivine occurs as euhedral microphenocrysts or rare corroded xenocrysts. In an EFS benmoreite the olivine is  $\text{Fo}_{49-43}$ .

CaO is low (0.12 wt.%) in the high-Mg phenocryst cores in basanite, suggesting crystallization at higher pressure than other lavas (Kohler & Brey, 1990). MnO increases from 0.12 wt.% in basanite to 2.56 wt.% in anorthoclase phonolite, most probably as a result of changing silica and iron activity in the melt (Watson, 1977; Takahashi, 1978).

#### *Clinopyroxene*

Clinopyroxene is ubiquitous in EL lavas as euhedral to subhedral fine- to medium-grained phenocrysts. It ranges from purplish brown in basanites to pale brown or greenish

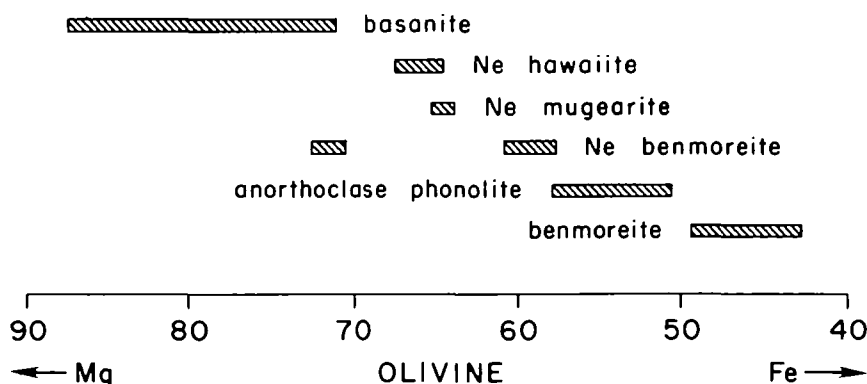


FIG. 2. Composition of olivine in various rock types from Mt. Erebus, plotted in terms of atomic % Mg and Fe.

brown in anorthoclase phonolites, and one sample had bright green aegirine-augite rims. Pyroxene phenocrysts show oscillatory zoning in the basanites and intermediate lavas but are unzoned in anorthoclase phonolites. In EFS lavas clinopyroxene is microporphyritic and euhedral, and is pale brown to brownish green in benmoreites to bright green in trachytes.

Compositions range from diopside to ferrosalite and ferroaugite (Table 2, Fig. 3), typical of alkaline igneous rocks (Wilkinson, 1956; Gibb, 1973). In EL lavas pyroxene phenocryst

TABLE 2

*Representative electron microprobe analyses of clinopyroxenes in Mt. Erebus lavas*

Rock Sample Position	Basanite 83435			Ne hawaite 83415		Ne benmoreite 25748	
	C	C	R	C	R	C	R
SiO <sub>2</sub>	46.50	43.35	46.79	47.70	47.32	49.40	49.30
TiO <sub>2</sub>	2.84	5.15	3.19	3.39	3.86	2.29	1.99
Al <sub>2</sub> O <sub>3</sub>	7.79	11.16	8.48	5.85	6.11	4.44	3.63
FeO*	9.91	7.12	6.52	7.67	7.84	8.55	8.35
MnO	0.25	—	—	0.21	0.27	0.49	0.51
MgO	11.09	11.77	13.25	12.41	12.10	12.10	12.40
CaO	20.25	22.17	22.12	21.65	21.23	21.80	23.10
Na <sub>2</sub> O	0.83	0.54	0.44	0.75	0.77	0.99	0.70
Sum	99.46	101.26	100.79	99.64	99.50	100.06	99.98
Fe <sub>2</sub> O <sub>3</sub>	1.89	2.82	1.89	1.26	0.44	2.23	3.41
FeO	8.21	4.58	4.82	6.54	7.44	6.54	5.28
Total	99.65	101.54	100.98	99.76	99.54	100.28	100.32
Ca	47.89	52.64	49.91	49.00	48.15	49.40	51.47
Mg	36.49	38.88	41.60	39.08	38.19	38.15	38.45
Fe <sup>2+</sup> + Mn	15.61	8.49	8.49	11.92	13.66	12.45	10.08

Rock Sample Position	Anorthoclase phonolite			Benmoreite AW82023 R	Phonolite inclusion 82431 GM
	83448		83400 OG		
	C	R			
SiO <sub>2</sub>	49.95	50.00	50.52	51.07	50.05
TiO <sub>2</sub>	1.91	1.84	1.21	0.86	1.64
Al <sub>2</sub> O <sub>3</sub>	4.14	3.69	1.10	2.03	4.68
FeO*	8.99	9.28	16.48	15.23	7.08
MnO	0.72	0.54	0.96	0.89	0.73
MgO	12.49	12.44	7.35	9.34	13.49
CaO	20.62	20.89	19.52	21.35	20.38
Na <sub>2</sub> O	1.01	0.99	1.41	0.57	1.53
Sum	99.83	99.67	98.55	101.34	99.58
Fe <sub>2</sub> O <sub>3</sub>	1.82	2.13	0.69	1.04	4.19
FeO	7.35	7.37	15.85	14.29	3.31
Total	100.01	99.88	98.62	101.44	100.00
Ca	46.54	47.07	45.52	46.21	48.17
Mg	39.22	39.01	23.85	28.13	44.36
Fe <sup>2+</sup> + Mn	14.24	13.92	30.63	25.67	7.47

\* Total Fe as FeO.

C—core; R—rim; GM—groundmass; OG—overgrowths.

Fe<sub>2</sub>O<sub>3</sub> and FeO partitioned using procedure of Papike *et al.* (1974).

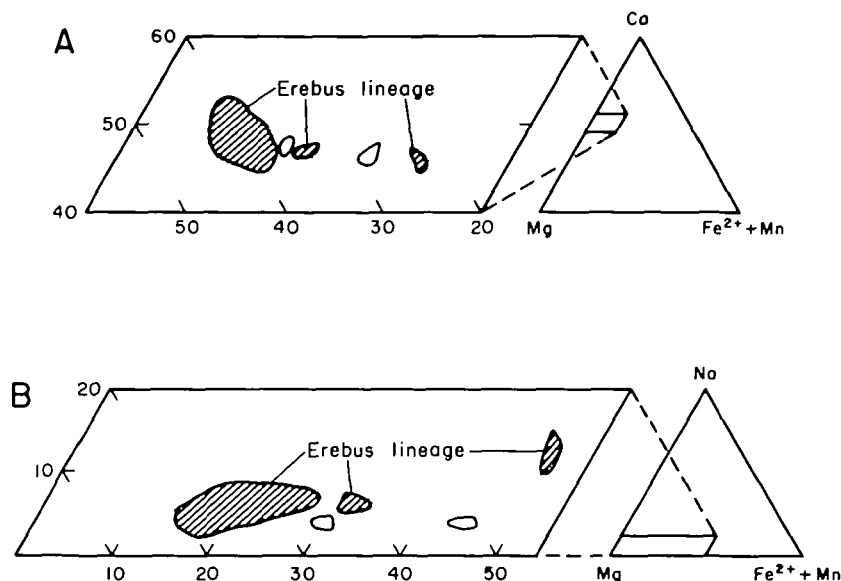


FIG. 3. Composition of clinopyroxene in samples from Mt. Erebus. Shaded fields are EL lavas; the two smaller shaded fields are groundmass and overgrowth clinopyroxenes in anorthoclase phonolite lavas. The open fields are EFS benmoreite (AW82023). (A) Plotted in terms of atomic % Ca, Mg,  $\text{Fe}^{2+}$  + Mn after charge balancing; (B) plotted in terms of atomic % Na, Mg,  $\text{Fe}^{2+}$  + Mn.

compositions show little variation and plot near the diopside–salite join. There is a slight decrease from  $\text{En}_{41}$  to  $\text{En}_{36}$  with magmatic evolution. Overgrowths and groundmass grains, especially in anorthoclase phonolite samples, are higher in Fe and Ca than phenocrysts. Clinopyroxenes in EFS benmoreite are enriched in  $\text{Fe}^{2+}$  relative to those in EL lavas.

Ti and Al are high in EL clinopyroxenes and decrease slightly with increasing sample differentiation. Some high-Al analyses plot above the CaMg–CaFe boundary as a result of high Ca-Tschermaks molecule ( $\text{CaAl}_2\text{SiO}_6$ ) contents. Most variation occurs in the basanite and Ne hawaiiite samples, where Al shows oscillatory zoning and usually decreases from core to rim. In the anorthoclase phonolites, Al increases from phenocryst cores to rims. Ti and Al are depleted in phenocryst overgrowths and groundmass clinopyroxenes. Clinopyroxene phenocrysts in EFS benmoreite have lower Ti and Al contents than those in EL lavas. The decreasing Al and Ti concentrations with increasing differentiation probably reflect changing Si, Ti, and Al activities in the melt as a result of concomitant clinopyroxene, Fe–Ti oxides, and plagioclase crystallization (Gibb, 1973; Kyle, 1981b). The drop in Al between the core and rim of pyroxene in basanite may also result from decreasing Ca-Tschermaks solubility because of declining pressure (Aoki, 1968). Higher Ti and Al in overgrowths and groundmass clinopyroxenes in some samples may be the result of enhanced solubility of Ca–Ti Tschermaks at low pressures (Aoki, 1968). The relatively low Ti and Al contents of clinopyroxenes from the EFS benmoreite suggests they crystallized from a melt with lower Ti and Al than EL magmas.

Na increases slightly in EL pyroxene phenocrysts as Fe content increases (Fig. 3). Overgrowths and groundmass pyroxenes in anorthoclase phonolite 83400 are enriched in  $\text{Fe}^{2+}$  and Na. Clinopyroxenes from EFS benmoreite AW82023 have low Na contents. The small Na enrichment trend in EL clinopyroxenes is similar to that of other strongly

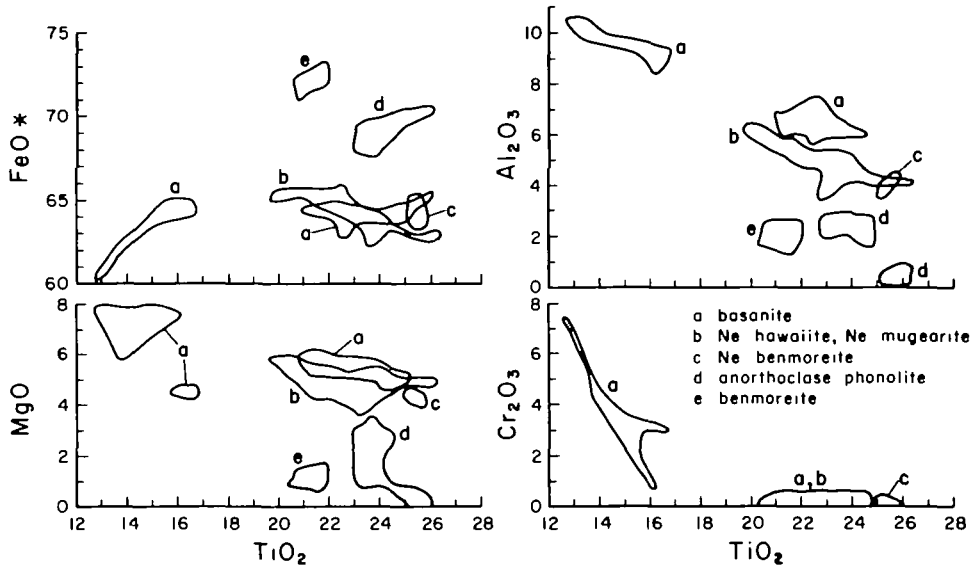


FIG. 4. Composition of opaque oxides in samples from Mt. Erebus. Variation of  $Al_2O_3$ ,  $Cr_2O_3$ ,  $MgO$ , and total Fe as  $FeO$  ( $FeO^*$ ) plotted against  $TiO_2$  (all in wt. %).

undersaturated differentiation sequences (e.g., South Qoroq nepheline syenites: Stephenson, 1972; DVDP lineage: Kyle, 1981b). Clinopyroxenes in the EFS benmoreite follow the trends of clinopyroxenes in less undersaturated sequences of the McMurdo Volcanic Group such as The Pleiades (Kyle, 1986) and the generalized alkali basalt–trachyte series from Japan (Aoki, 1964).

The lack of strong  $Fe^{3+}$  and Na enrichment in EL pyroxenes suggests that oxygen fugacity was constant during differentiation. The continuous crystallization of olivine with increasing Fe contents and magnetite may have buffered  $f_{O_2}$ . The Na enrichment in groundmass clinopyroxenes from anorthoclase phonolite 83400 probably resulted from higher oxygen fugacity during cooling after eruption of the lavas.

#### Opaque oxides

Titanomagnetite is common as a phenocryst and groundmass phase in all lavas. Corroded phenocrysts in basanite 83435 are chromian magnetites (4.60–7.40 wt.%  $Cr_2O_3$ ) (Fig. 4). Rare ilmenite phenocrysts occur in Ne hawaiiites and Ne benmoreites.

$Al_2O_3$  and  $MgO$  decrease and  $FeO$  and  $MnO$  increase in EL magnetites with increasing sample differentiation (Fig. 4). The titaniferous magnetites from Mt. Erebus are typical of alkaline igneous suites (Haggerty, 1976).

Using magnetite and ilmenite (Stormer, 1983), temperatures and  $\log f_{O_2}$  in Ne hawaiiites AW82038 and 83415 average  $1081 \pm 12^\circ C$  and  $-9.99 \pm 0.15$ , respectively. These values fall on the quartz–fayalite–magnetite (QFM) oxygen buffer curve, characteristic of extrusive basaltic rocks (Haggerty, 1976).

#### Pyrrhotite

Pyrrhotite is common in anorthoclase phonolites as small blebs within or contacting magnetite grains, but occasionally as microphenocrysts. In an Ne hawaiiite the pyrrhotite has a molecular  $FeS$  content of 0.96–1.00.

Using a temperature of 1081 °C and an average atomic percentage FeS value of 0.98 in pyrrhotites, the  $\log f_{S_2}$  of the Ne hawaiiite magma is  $-3.01$  (Toulmin & Barton, 1964). This is identical to the  $\log S_2$  fugacity of gas from Kilauea volcano, Hawaii (Heming & Carmichael, 1973), and lower than the value ( $-2.75$ ) calculated at 1000 °C for anorthoclase phonolite ejecta from Mt. Erebus (Kyle, 1977).

### Feldspar

Feldspar is the dominant phenocryst phase in Erebus lavas. Plagioclase occurs as euhedral, fine-grained, unzoned phenocrysts in basanites, and as euhedral or subhedral oscillatory zoned phenocrysts up to 3 cm in length in intermediate lavas of the EL. Resorbed cores and embayed rims are common. Anorthoclase phonolites contain euhedral, unzoned anorthoclase phenocrysts up to 5 cm in length and form up to 40% of the mode. In EFS lavas feldspar occurs as subhedral to euhedral fine-grained phenocrysts or microphenocrysts.

In EL lavas feldspar ranges from  $An_{72}$  in basanites to  $Or_{54}$  in the groundmasses of some Ne mugearite and anorthoclase phonolites samples (Fig. 5). Microphenocrysts and phenocrysts are similar in composition and are more calcic than groundmass feldspar. The abundant rhomb-shaped phenocrysts in the anorthoclase phonolites range from  $An_{28}Or_{16}$  (oligoclase) in the less evolved anorthoclase phonolite samples (e.g., 83446) to  $An_{10}Or_{25}$  (anorthoclase) (Fig. 5) in the more evolved samples (e.g., 80020) and recent ejecta (Kyle,

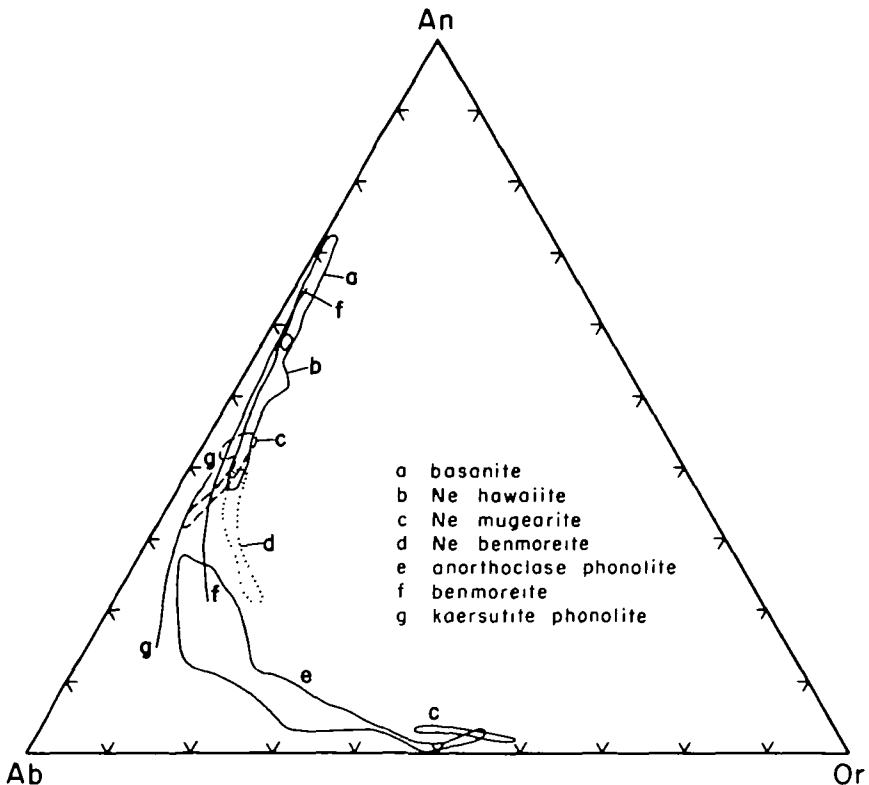


FIG. 5. Composition of feldspars in various rock types within the EL.

1977). There is minor variation in  $Ab_{65-71}$  and zoning is limited to slight variations in An and Or. The phenocrysts sometimes have thin discontinuous sanidine rims ( $Or_{37-38}$ ). Groundmass feldspars range from anorthoclase to sanidine.

Feldspar in the EL forms a continuous trend, whereas feldspar in EFS benmoreite AW82023 is more albitic, suggesting a different evolutionary path for these lavas. Similar divergent feldspar trends have been observed at other volcanic centers (e.g., Gough Island: Le Roex, 1985; Mt. Kenya: Price *et al.*, 1985). The higher albite content of feldspar from the EFS benmoreite may be due to its increased stability at higher water contents (Tuttle & Bowen, 1958).

Rare earth and trace elements were analyzed in three andesines and an oligoclase separated from Ne hawaiiite and Ne benmoreite (Table 3). The feldspar has low rare earth element (REE) concentrations, and enriched light REE and Eu, typical of feldspars. Calculated feldspar/whole-rock and feldspar/groundmass partition coefficients (Table 3) are typical of intermediate lavas (Schnetzler & Philpotts, 1970).

#### *Feldspathoids, sodalite, and apatite*

EL lavas are strongly undersaturated, containing up to 24% normative Ne. Rare nepheline microphenocrysts and sodalite-pyroxene microxenoliths occur in some Ne hawaiiite samples. Minor amounts of feldspathoids were observed in the groundmass of basanites and intermediate lavas. Anorthoclase phonolites contain groundmass sodalite and nepheline. Feldspathoids were not observed in the EFS lavas.

Microphenocrysts of apatite are common in most rocks.

### GEOCHEMISTRY

Major, trace, and rare earth elements were measured by X-ray fluorescence (XRF) (Norrish & Chappell, 1977) and instrumental neutron activation analysis (INAA) (Jacobs *et al.*, 1977; Lindstrom & Korotev, 1982). Sr and Nd isotope analyses were carried out using standard separation procedures, and employed a multidynamic 5-collector technique on a VG354 mass spectrometer. During the period of analysis, Sr standard SRM 987 had an  $^{87}Sr/^{86}Sr$  value of  $0.710249 \pm 19$  (2 S.D.,  $n = 36$ ). Internal precision for single analyses is  $\pm 0.00001$  (2 S.E.). All data are normalized to an  $^{86}Sr/^{88}Sr$  value of 0.1194.

All samples are undersaturated, with 5–24% Ne, except the EFS trachytes which are slightly undersaturated (0.7% Ne) to oversaturated (0.4–2.1% Qz). EL lavas form continuous major element trends on silica variation diagrams (Figs. 1 and 6). Minor scatter is seen, especially for  $Al_2O_3$ , as a result of feldspar accumulation.  $TiO_2$ , MgO, CaO, and  $P_2O_5$  decrease with increasing  $SiO_2$ . In EL lavas  $Al_2O_3$ ,  $Na_2O$ , and  $K_2O$  increase up to ~52%  $SiO_2$ ,  $Al_2O_3$  then decreases, and the trends of  $Na_2O$  and  $K_2O$  level out. Anorthoclase phonolites show only slight variation in major element compositions. EFS lavas are distinctly higher in  $FeO^*$  and depleted in  $Al_2O_3$ ,  $Na_2O$ , and  $K_2O$  compared with EL lavas.

EL lavas exhibit smooth continuous trace element trends (Fig. 7) similar to the major elements. There are strong enrichments of incompatible elements such as Rb, Zr, and Th. Compatible elements such as V, Cr, and Sr decrease with differentiation.

EL lavas have high concentrations of REE (Fig. 8A) and are LREE enriched ( $La_N/Yb_N = 13.5-20.2$ ). With differentiation the HREE are enriched relative to the LREE, as shown by decreasing La/Yb (Fig. 7). Some Ne hawaiiite and anorthoclase phonolite samples have slight positive Eu anomalies.

TABLE 3

Analyses of plagioclase separates and associated whole-rock and groundmass of EL rock samples

Sample	1			2			3			4		
	Plag.	WR	GM									
FeO*	0.54	9.18	10.96	0.65	8.41	10.92	0.35	8.06	9.73	0.32	6.77	7.06
Na <sub>2</sub> O	4.86	6.68	5.59	5.85	5.60	5.69	5.02	6.26	6.81	6.46	—	7.61
Sc	0.3	6.9	7.7	0.3	6.1	7.8	0.1	5.1	5.3	0.1	5.3	5.9
Cr	<1	7	8	<1	3	<2	<1	<2	<2	<1	<2	<2
Rb	3	59	70	4	54	68	<3	55	81	5	86	114
Cs	0.04	0.54	0.59	0.07	0.60	0.65	<0.04	0.48	0.70	<0.04	0.89	1.20
Ba	514	793	708	505	694	813	639	980	975	1365	944	879
La	14.0	95.9	106.5	16.0	88.8	109.7	15.0	89.5	104.7	27.1	—	131.0
Ce	20.0	138.2	208.6	25.0	174.4	218.0	21.0	176.0	203.5	35.0	215.0	253.6
Sm	0.9	14.1	15.7	1.2	12.9	16.2	0.8	12.8	14.4	1.3	—	16.4
Eu	2.39	4.20	4.39	2.42	4.03	4.57	3.16	4.24	4.13	4.26	3.99	3.92
Tb	0.07	1.34	1.54	0.09	1.52	1.72	0.06	1.60	1.51	0.11	1.65	1.79
Yb	<0.2	3.5	4.2	0.2	3.3	4.3	<0.2	3.8	4.2	<0.2	4.6	5.6
Lu	0.02	0.44	0.56	<0.02	0.46	0.56	<0.02	0.52	0.66	0.22	—	0.78
Hf	0.3	8.8	10.0	0.4	8.1	10.3	0.1	9.1	11.4	0.3	14.1	17.7
Ta	0.4	10.0	10.9	0.4	8.5	11.0	0.1	9.7	12.2	0.2	13.1	15.9
Th	0.3	11.8	13.3	0.5	10.7	13.8	0.1	10.6	13.6	0.4	16.9	21.5
U	<1	3.9	3.9	<1	3.6	4.8	<1	5.0	4.4	<1	—	7.2
<i>Distribution coefficients</i>												
Sc		0.043	0.039		0.049	0.039		0.020	0.019		0.019	0.017
Rb		0.055	0.045		0.075	0.059		—	—		0.059	0.044
Cs		0.074	0.068		0.117	0.108		—	—		—	—
Ba		0.648	0.726		0.728	0.621		0.652	0.655		1.446	1.553
La		0.146	0.131		0.180	0.146		0.168	0.143		—	0.207
Ce		0.106	0.096		0.143	0.115		0.119	0.103		0.163	0.138
Sm		0.064	0.057		0.093	0.074		0.063	0.056		—	0.079
Eu		0.569	0.544		0.600	0.529		0.745	0.765		1.068	1.087
Tb		0.052	0.045		0.059	0.052		0.037	0.040		0.067	0.061
Yb		—	—		0.061	0.046		—	—		—	—
Lu		0.045	0.036		—	—		—	—		—	0.026
Hf		0.034	0.030		0.049	0.039		0.011	0.009		0.021	0.017
Ta		0.040	0.037		0.047	0.036		0.010	0.008		0.015	0.013
Th		0.025	0.023		0.047	0.036		0.009	0.007		0.024	0.019

Calculated feldspar/whole-rock and feldspar/groundmass distribution coefficients are given below the analyses. Oxides are given in wt.%, trace elements in ppm.

All analyses by instrumental neutron activation analysis; —not analyzed. Plag.—plagioclase; WR—whole rock; GM—groundmass.

All plagioclase is andesine, except sample 4 which is oligoclase. 1, Ne hawaiiite (25754), Turks Head; 2, Ne hawaiiite (25758), Tryggve Point; 3, Ne hawaiiite (25778),

Fang Ridge; 4, Ne benmoreite (25748), Tent Island.

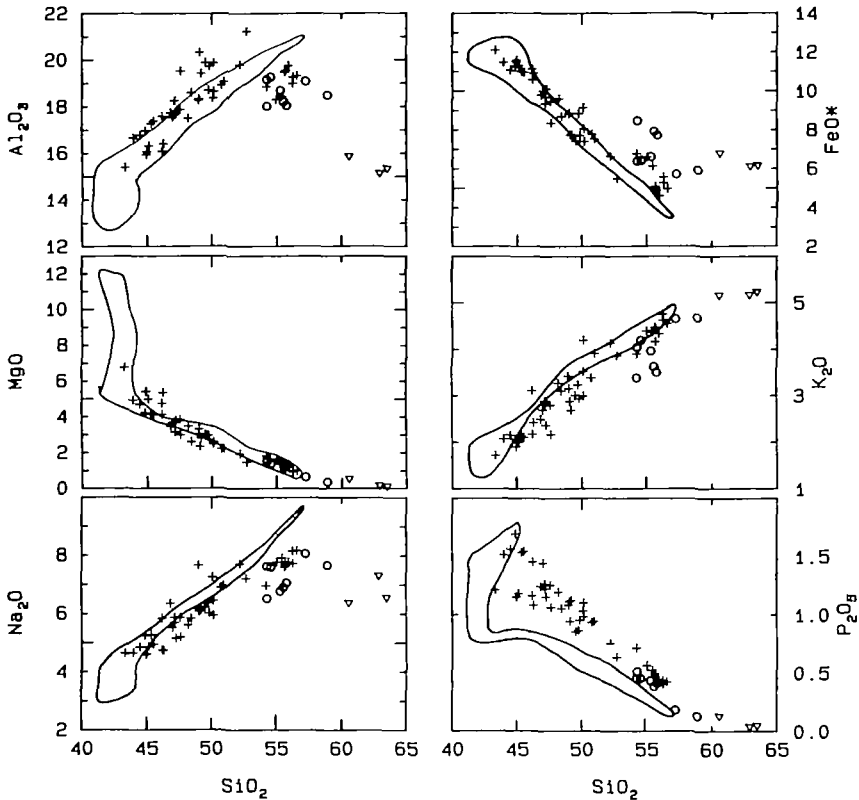


FIG. 6. Variation of major element oxides in samples from Mt. Erebus, as plotted against silica. +, EL lavas; O, EFS lavas;  $\nabla$ , trachyte. Open fields are DVDP lineage rocks. All values in wt. %.

EFS benmoreites have lower REE concentrations than EL lavas (Fig. 8A). The EFS trachytes have the highest REE concentrations and large negative Eu anomalies.

$^{87}\text{Sr}/^{86}\text{Sr}$  ratios are uniformly low (0.70294–0.70303) in all EL lavas (Table 4). An EFS benmoreite from Inaccessible Island is isotopically similar to the EL lavas, whereas a trachyte from Aurora Cliff has a higher  $^{87}\text{Sr}/^{86}\text{Sr}$  of 0.70425. An anorthoclase phonolite sample (80020) has a  $^{143}\text{Nd}/^{144}\text{Nd}$  ratio of  $0.512912 \pm 4$  (normalized to an  $^{146}\text{Nd}/^{144}\text{Nd}$  value of 0.7219). Additional isotopic data on samples from Mt. Erebus have been given by Sun & Hanson (1975), Stuckless & Ericksen (1976), and Jones *et al.* (1983).

The  $^{87}\text{Sr}/^{86}\text{Sr}$  ratios are low, within the low end of the range exhibited by oceanic island basalts (Zindler & Hart, 1986).  $^{206}\text{Pb}/^{204}\text{Pb}$  ranges from 19.4 to 20.1 in Mt. Erebus and other Ross Island samples (Sun & Hanson, 1975). The radiogenic Pb and unradiogenic Sr isotope data suggest that Ross Island basanites were derived from a mantle source reservoir with a high proportion of HIMU component (Zindler & Hart, 1986).

## PETROGENESIS

### *Evolution of the Erebus lineage*

EL lavas range from basanite to anorthoclase phonolite and define single trends on geochemical variation diagrams (Figs. 6 and 7), indicating that the lineage evolved from a

basanite parental magma. The evolution of igneous suites by fractional crystallization is characterized by decreasing compatible trace elements whereas incompatible elements increase and have constant ratios with each other. EL lavas form smooth geochemical trends, and show similar incompatible element ratios (e.g., Zr/Nb 2.7–3.6, Ba/Rb 9.6–11.7), in strong support of evolution by fractional crystallization.

The progressive decrease of TiO<sub>2</sub>, FeO\*, MgO, CaO, and P<sub>2</sub>O<sub>5</sub> with increasing evolution of EL lavas is indicative of olivine, clinopyroxene, opaque oxide, and apatite fractionation. The Al<sub>2</sub>O<sub>3</sub>, Na<sub>2</sub>O, and K<sub>2</sub>O trends suggest that feldspar fractionation occurred in lavas more evolved than Ne benmoreite.

Trace element trends in the EL can also be explained by fractional crystallization (Fig. 7). Sc, Y, Cr, Ni, and Cu decline sharply in the more basic rocks to detection limits, most

TABLE 4  
*Representative analyses of volcanic rocks from Mt. Erebus*

	1	2	3	4	5	6	7
SiO <sub>2</sub>	43.32	43.97	44.50	44.89	46.20	47.19	48.22
TiO <sub>2</sub>	3.78	3.75	3.690	3.20	3.16	2.72	2.60
Al <sub>2</sub> O <sub>3</sub>	15.38	16.65	16.77	16.96	16.07	18.24	17.49
FeO*	12.08	11.44	11.04	11.23	11.11	9.33	9.58
MnO	0.22	0.24	0.25	0.23	0.25	0.22	0.23
MgO	6.77	4.92	4.69	4.21	4.74	3.13	3.47
CaO	10.66	9.62	9.71	9.28	8.05	7.52	6.79
Na <sub>2</sub> O	4.63	4.64	4.84	5.24	4.74	5.89	5.61
K <sub>2</sub> O	1.72	2.07	2.15	2.07	3.11	2.83	3.27
P <sub>2</sub> O <sub>5</sub>	1.21	1.51	1.56	1.69	1.16	1.22	1.19
LOI	0.03	-0.44	-0.56	-0.13	0.33	0.78	0.17
Total	99.82	98.36	98.61	98.88	98.91	99.05	98.63
Sc	20.3	11.1	11.2	8.82	13.15	6.42	9.11
Y	291	192	179	138	147	73	97
Cr	130	27	9	2	61	2	25
Ni	63	13	10	<5	27	10	13
Cu	43	23	22	19	46	56	31
Zn	104	112	113	123	124	111	114
Ga	21	22	21	22	24	22	24
As	<1.0	<1.0	<1.0	1.6	<1.0	1.2	1.8
Rb	41	41	41	46	62	61	72
Sr	1100	1374	1386	1421	871	1295	1123
Y	37	41	44	45	48	46	46
Zr	363	347	358	427	522	482	540
Nb	111	126	131	145	158	163	183
Sb	0.1	0.1	0.1	0.1	—	0.1	0.1
Cs	0.38	0.40	0.40	0.44	0.53	0.62	0.70
Ba	485	653	682	593	686	721	763
La	70.0	77.0	79.3	92.0	89.5	94.7	100.2
Ce	149.8	164.5	170.1	198.4	189.5	195.3	205.7
Nd	67	76	85	98	85	86	91
Sm	12.45	13.80	13.93	14.87	15.11	14.46	13.72
Eu	3.63	4.07	4.12	4.42	3.96	4.01	3.90
Tb	1.33	1.57	1.55	1.68	1.75	1.64	1.65
Yb	2.55	2.86	3.17	3.20	3.43	3.35	3.49
Lu	0.40	0.44	0.48	0.49	0.57	0.51	0.54
Hf	8.49	7.65	7.87	9.19	10.6	9.78	11.1
Ta	6.57	7.32	7.50	8.27	8.92	9.46	10.4
Pb	<4	<4	<4	<4	<4	<4	<4
Th	7.2	6.6	7.1	8.4	10.0	11.3	12.3
U	1.6	1.9	2.0	2.5	2.1	3.2	3.1
<sup>87</sup> Sr/ <sup>86</sup> Sr	0.702958	0.702977	0.702977	0.702937	0.703021		0.702992

probably because of olivine, clinopyroxene, and opaque oxide fractionation. Sr increases slightly from basanite to Ne-hawaiiite, then declines to anorthoclase phonolite, suggesting apatite and feldspar fractionation from lavas more evolved than Ne hawaiiite. Ga, Y, Zr, Nb, Cs, Ba, Hf, Ta, Th, and U increase in concentration in the lavas from basanite to anorthoclase phonolite. This is consistent with fractionation of olivine, clinopyroxene, opaque oxides, feldspar, and apatite. Rb increases from basanite to Ne benmoreite, then levels out in the anorthoclase phonolite. The anorthoclase is enriched in Rb (Mason *et al.*, 1982) and if fractionated would result in lowering Rb contents.

Fractional crystallization can explain the REE patterns of the EL. The overall enrichment of REE is limited, largely as a result of apatite fractionation. Middle REE show almost no change in concentration, as a result of clinopyroxene and apatite fractionation. Small positive Eu anomalies in some samples suggest that they may contain minor

TABLE 4 (Continued)

	8	9	10	11	12	13	14
SiO <sub>2</sub>	49.53	50.17	50.77	54.22	55.00	55.63	55.93
TiO <sub>2</sub>	2.12	2.18	1.95	1.58	1.36	1.18	1.10
Al <sub>2</sub> O <sub>3</sub>	19.87	18.64	18.91	18.84	18.29	19.46	19.74
FeO*	7.41	8.04	7.78	6.76	6.59	5.06	4.59
MnO	0.17	0.22	0.22	0.23	0.27	0.20	0.18
MgO	3.00	2.51	2.20	1.81	1.64	1.30	1.23
CaO	6.93	5.73	5.55	4.22	3.34	3.16	3.20
Na <sub>2</sub> O	6.22	6.44	6.90	6.96	7.77	7.60	7.77
K <sub>2</sub> O	3.00	3.52	3.38	3.90	4.39	4.47	4.33
P <sub>2</sub> O <sub>5</sub>	0.85	1.10	0.93	0.71	0.56	0.46	0.44
LOI	-0.22	-0.01	0.17	-0.12	-0.28	0.03	0.15
Total	98.89	98.53	98.76	99.10	98.92	98.55	98.66
Sc	7.06	6.32	5.09	4.25	4.90	3.06	2.80
V	95	62	37	24	35	19	13
Cr	33	<2	<2	<2	3	2	2
Ni	13	7	7	7	9	6	7
Cu	31	19	21	11	13	10	10
Zn	82	96	108	124	153	108	99
Ga	23	23	24	26	28	28	27
As	1.7	1.1	2.1	<1.0	<1.0	2.0	<1.0
Rb	70	77	75	86	101	107	99
Sr	1345	1270	1188	1171	744	885	990
Y	33	46	47	53	68	55	49
Zr	448	632	608	766	942	927	855
Nb	160	179	192	214	259	255	236
Sb	0.1	0.2	0.1	0.2	0.2	0.3	0.3
Cs	0.69	0.74	0.83	0.98	1.12	1.37	1.20
Ba	730	819	909	990	1050	1010	1064
La	74.9	101.2	107.9	111.0	134.4	109.2	103.9
Ce	148.8	207.7	218.1	222.9	273.7	218.8	204.2
Nd	57	91	95	96	114	85	80
Sm	9.70	13.91	13.89	14.43	17.58	13.31	12.02
Eu	3.06	3.94	4.11	4.48	5.17	4.21	4.27
Tb	1.16	1.65	1.70	1.78	2.20	1.74	1.57
Yb	2.48	3.76	3.95	4.70	5.96	4.87	4.74
Lu	0.39	0.57	0.59	0.70	0.87	0.77	0.71
Hf	8.43	13.2	12.6	16.8	20.9	19.9	18.1
Ta	9.18	10.7	11.3	12.6	15.0	14.9	13.7
Pb	<4	<4	<4	<4	<4	5	<4
Th	12.0	13.4	13.9	15.4	18.1	18.9	17.5
U	3.3	4.4	4.7	4.8	6.4	5.6	5.2
<sup>87</sup> Sr/ <sup>86</sup> Sr	0.702959	0.702990	0.703000	0.703027			

TABLE 4 (Continued)

	15	16	17	18	19	20	21	22	23	24
SiO <sub>2</sub>	56.27	56.57	54.28	55.81	58.91	60.59	63.51	52.69	55.04	41.68
TiO <sub>2</sub>	0.99	0.98	1.20	1.07	0.44	0.74	0.43	2.18	1.19	4.06
Al <sub>2</sub> O <sub>3</sub>	19.25	19.31	18.01	18.03	18.47	15.85	15.33	19.04	20.06	12.92
FeO*	5.26	4.95	8.46	7.71	5.89	6.79	6.15	7.52	5.13	11.23
MnO	0.23	0.23	0.29	0.30	0.26	0.22	0.21	0.24	0.18	0.18
MgO	0.95	0.99	1.57	1.35	0.37	0.56	0.14	2.50	1.14	12.13
CaO	2.78	2.75	4.40	3.75	2.19	1.94	1.44	5.98	3.73	11.32
Na <sub>2</sub> O	7.72	8.17	6.52	7.06	7.66	6.38	6.56	5.90	7.44	3.16
K <sub>2</sub> O	4.62	4.55	3.38	3.50	4.67	5.16	5.23	2.15	4.00	1.48
P <sub>2</sub> O <sub>5</sub>	0.40	0.42	0.51	0.41	0.13	0.13	0.05	1.13	0.47	0.84
LOI	0.12	-0.21	0.01	-0.22	0.03	0.07	0.18	-0.05	0.19	—
Total	98.60	98.72	98.62	98.75	99.02	98.42	99.23	99.26	98.57	99.31†
Sc	3.02	2.58	2.20	2.07	0.58	5.47	2.79	4.81	2.87	—
V	11	12	10	10	12	<10	<10	48	18	300
Cr	2	<2	<2	<2	<2	<2	<2	2	<2	469
Ni	6	7	6	7	6	7	9	7	7	276
Cu	<10	10	13	10	10	<10	<10	13	<10	52
Zn	112	130	134	122	123	176	269	97	85	82
Ga	28	29	25	25	25	31	33	24	26	—
As	<1.0	<1.0	<1.0	<1.0	<1.0	3.8	1.9	<1.0	5.0	—
Rb	105	102	75	80	109	132	161	44	88	30
Sr	851	878	970	923	381	81	13	1643	1081	829
Y	60	64	42	43	40	71	92	51	49	33
Zr	935	946	628	634	848	969	1085	458	948	—
Nb	247	261	172	193	201	232	258	140	251	80
Sb	0.3	0.3	0.3	0.2	0.3	0.3	0.5	—	0.2	—
Cs	1.14	1.27	0.70	0.73	1.07	1.94	3.69	0.41	0.80	0.31
Ba	1144	1164	887	1109	1321	811	304	1205	889	277
La	120.7	126.9	111.5	113.0	119.3	132.2	164.9	117.2	97.7	53
Ce	242.7	252.7	217.7	228.4	220.9	268.4	325.1	234.6	194.4	>110
Nd	101	97	86	88	74	109	145	106	78	49
Sm	14.98	15.25	11.94	12.22	10.13	17.03	21.00	15.84	12.13	9.2
Eu	4.83	4.97	3.51	3.83	2.80	3.36	2.91	5.50	3.86	2.7
Tb	1.91	1.99	1.35	1.44	1.20	2.18	2.87	1.80	1.56	0.94
Yb	5.55	5.64	3.64	3.93	3.99	6.31	7.88	3.92	4.83	1.6
Lu	0.85	0.84	0.56	0.61	0.64	0.93	1.17	0.58	0.73	—
Hf	20.6	20.6	13.8	13.9	17.5	21.5	25.2	10.6	20.1	5.8
Ta	14.9	15.0	10.4	11.4	12.5	12.5	14.6	8.97	14.2	—
Pb	<4	<4	<4	6	12	16	31	<4	<4	8.0
Th	19.2	18.6	12.9	14.3	18.4	21.4	25.4	9.8	20.0	4.7
U	4.6	5.9	3.3	4.8	4.8	6.9	7.9	2.9	6.8	1.2
<sup>87</sup> Sr/ <sup>86</sup> Sr		0.703029	0.703029	0.703003		0.704248				

Major elements are given in wt. %, trace elements in ppm.

1, Basanite (83435), Cape Barne; 2, basanite (83437), Fang Ridge; 3, basanite (79300), Cape Barne; 4, Ne hawaiiite (83432), Cape Barne; 5, Ne hawaiiite (AW82044), Turks Head; 6, Ne hawaiiite (AW82038), Turks Head; 7, Ne hawaiiite (83409), Inaccessible Island; 8, Ne hawaiiite (83415), Tent Island; 9, Ne mugearite (83417), Tent Island; 10, Ne benmoreite (83410), Inaccessible Island; 11, Ne benmoreite (AW82015), Turks Head; 12, anorthoclase phonolite (83452), Bomb Peak; 13, anorthoclase phonolite (83446), Cape Royds; 14, anorthoclase phonolite (83448); 15, anorthoclase phonolite (83400), Mt. Erebus; 16, anorthoclase phonolite (80020), Three Sisters Cone; 17, benmoreite (83412), Inaccessible Island; 18, benmoreite (AW82023), Lewis Bay; 19, phonolite (83407), Inaccessible Island; 20, trachyte (83454), Aurora Cliffs; 21, trachyte (82405), Bomb Peak; 22, cumulate xenolith (82403), summit, Mt. Erebus; 23, anorthoclase phonolite xenolith (82431), Bomb Peak; 24, basanite, assumed to be parental for the Erebus lineage, from Dry Valley Drilling Project hole 2, Hut Point Peninsula (2–105.53) from Kyle (1981b).

† Includes Fe<sub>2</sub>O<sub>3</sub> = 3.06, FeO = 8.48.

LOI, loss on ignition.

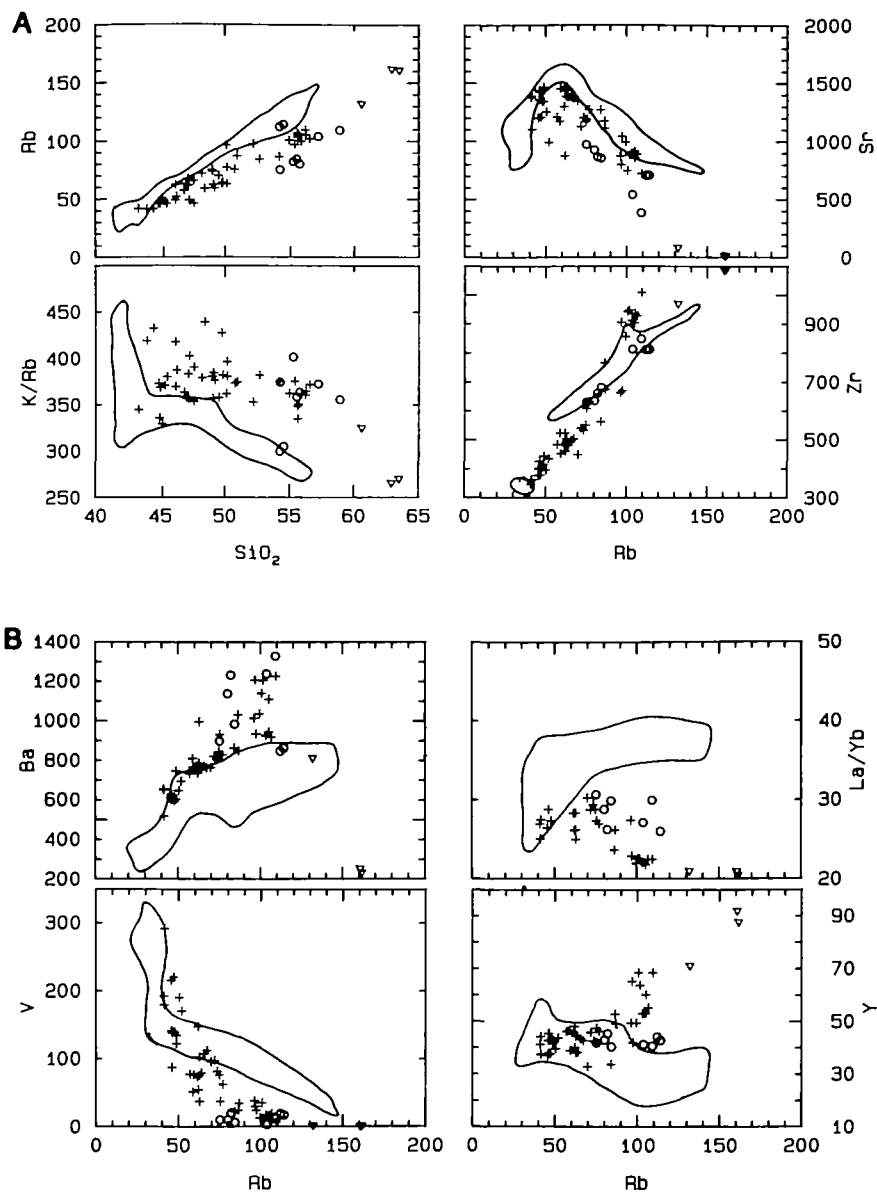


FIG. 7. Variation of selected trace elements in samples from Mt. Erebus and comparison with trends in the DVDP lineage shown by fields. +, EL lavas; O, EFS lavas;  $\nabla$ , trachytes.

cumulate feldspar. Large Eu anomalies are absent. Fractionation of feldspar similar to those analyzed in Table 3 would result in negative Eu anomalies, suggesting that feldspar fractionation was minor. However, depletion of Eu by feldspar fractionation may have been balanced out by enrichment of Eu as a result of clinopyroxene and apatite fractionation.

The near-uniform  $^{87}Sr/^{86}Sr$  values of the EL lavas (Table 4) show that crustal contamination is unlikely to have had any significant effect on the major and trace element abundances of the rocks.

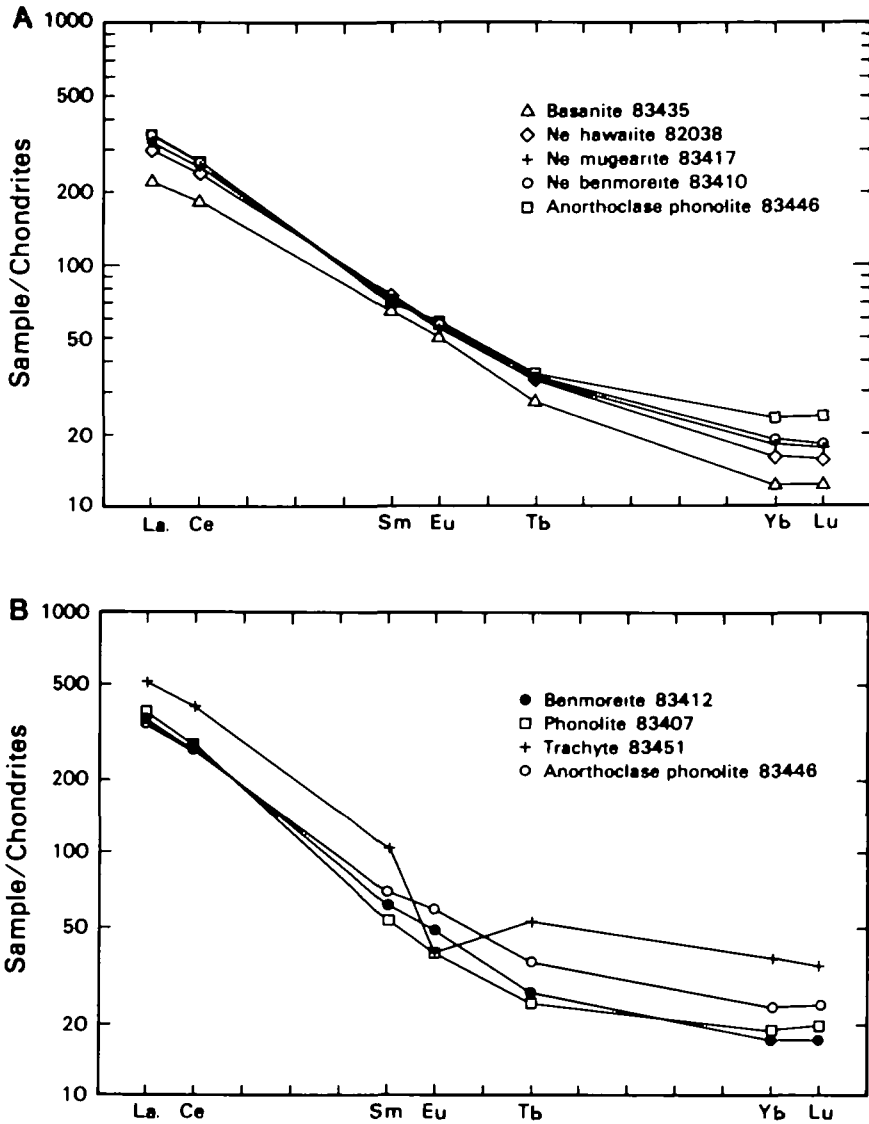


FIG. 8. Chondrite-normalized REE plots of Erebus rocks, using normalizing factors of Taylor & Gorton (1977). (A) Representative EL samples. (B) Representative EFS samples, including a typical EL anorthoclase phonolite for comparison.

*Fractionation sequence*

Quantitative crystal fractionation models for the EL were made by least-squares mass balance methods using major elements (Bryan *et al.*, 1969). Microprobe analyses of phenocrysts from the samples were used. Additional analyses of a chrome spinel (Kyle, 1981b), nepheline (Deer *et al.*, 1966), and apatite (P. R. Kyle, unpub. data) were included. Geologically and mineralogically reasonable models with sums of squares of differences of <0.1 were accepted, and were tested using trace element data and the Rayleigh fractionation equation (Arth, 1976). Empirical mineral/melt partition coefficients from the literature and Table 3 were used in the modeling.

A primitive basanite (2-105-53) (Kyle, 1981b) from a DVDP drill core was used as the parental magma for the Erebus lineage. Primitive basanites are unknown on Mt. Erebus, and extrapolation of major and trace element trends (Figs. 6 and 7) for EL lavas coincided with the basanite. In addition, incompatible element ratios were similar in the DVDP basanite and the more evolved basanites from Mt. Erebus. Evolution of the EL was modeled in three steps.

Evolution from basanite to Ne hawaiiite gave three solutions (Table 5). In addition to the main phenocryst phases, Cr spinel was fractionated in models 1 and 2, and in models 2 and 3 nepheline and nepheline and feldspar were also fractionated, respectively. Model 1 has predicted trace element concentrations similar to those observed, with the exceptions of Sr and Ba. This may be due to uncertainties in the distribution coefficients for these elements. Predicted trace element concentrations are too high in models 2 and 3, suggesting that these models are less likely.

Two models for Ne hawaiiite to Ne benmoreite evolution (Table 6) are similar, except one

TABLE 5

*Least-squares mass balance models for derivation of Ne hawaiiite (AW82038) from basanite (2-105-53)*

	<i>Observed basanite</i>	<i>1</i>	<i>Estimated basanite</i>	
			<i>2</i>	<i>3</i>
SiO <sub>2</sub>	42.06	42.10	42.06	42.07
TiO <sub>2</sub>	4.21	4.21	4.21	4.21
Al <sub>2</sub> O <sub>3</sub>	13.08	13.09	13.08	13.07
FeO*	11.46	11.46	11.46	11.46
MnO	0.18	0.21	0.20	0.19
MgO	12.11	12.08	12.11	12.10
CaO	11.50	11.44	11.49	11.49
Na <sub>2</sub> O	3.03	2.88	3.08	3.13
K <sub>2</sub> O	1.51	1.31	1.38	1.32
P <sub>2</sub> O <sub>5</sub>	0.87	0.94	0.88	0.88
Wt. fraction Ne hawaiiite		0.4547	0.4133	0.3475
Olivine	(Fo <sub>88</sub> B)	0.1163	0.1166	0.1299
Clinopyroxene	(En <sub>41</sub> B)	0.3466	0.3643	0.3473
Cr spinel	(Usp <sub>8</sub> B)	0.0354	0.0261	—
Ti magnetite	(Usp <sub>52</sub> B)	0.0124	0.0214	0.0438
Ilmenite		0.0236	0.0226	0.0238
Feldspar	(An <sub>72</sub> B)	—	—	0.0518
Nepheline	(Ne1)	—	0.0272	0.0453
Apatite		0.0092	0.0088	0.0107
Sum		0.9982	1.0002	1.0001
Sum R <sup>2</sup> *		0.07	0.02	0.05
<i>Trace element abundances (ppm) in Ne hawaiiite</i>				
	<i>Observed</i>			<i>Calculated</i>
Rb	62	65	71	84
Sr	1295	1663	1822	1829
Nb	163	160	175	207
Ba	721	598	658	766
La	95	99	109	125
Ce	195	194	212	240
Sm	14.5	13.7	14.8	16.4
Eu	4.0	4.3	4.6	5.0
Yb	3.4	3.5	3.8	4.3
Lu	0.5	0.5	0.5	0.6

\* R<sup>2</sup> is the square of the residuals.

TABLE 6

*Least-squares mass balance models for derivation of Ne benmoreite (83410) from Ne hawaiiite (AW82038)*

	Observed	Estimated Ne hawaiiite	
	Ne hawaiiite	1	2
SiO <sub>2</sub>	48.03	48.09	48.04
TiO <sub>2</sub>	2.76	2.73	2.75
Al <sub>2</sub> O <sub>3</sub>	18.57	18.51	18.54
FeO*	9.50	9.52	9.51
MnO	0.23	0.22	0.22
MgO	3.19	3.10	3.17
CaO	7.65	7.61	7.65
Na <sub>2</sub> O	5.96	5.83	6.09
K <sub>2</sub> O	2.88	2.70	2.69
P <sub>2</sub> O <sub>5</sub>	1.24	1.30	1.24
Wt. fraction Ne benmoreite		0.7790	0.6880
Olivine	(Fo <sub>66</sub> Nh)	0.0117	(Fo <sub>65</sub> Nh) 0.0121
Clinopyroxene	(En <sub>40</sub> B)	0.0624	(En <sub>39</sub> Nh) 0.0788
Ti magnetite	(Usp <sub>73</sub> Nh)	0.0399	(Usp <sub>71</sub> Nh) 0.0479
Feldspar	(An <sub>64</sub> B)	0.0904	(An <sub>52</sub> Nh) 0.1221
Nepheline		—	(Nel) 0.0377
Apatite		0.0136	0.0144
Sum		0.9970	1.0010
Sum R <sup>2</sup> *		0.07	0.06
<i>Trace element abundances (ppm) in Ne benmoreite</i>			
	<i>Observed</i>		<i>Calculated</i>
Rb	72	79	89
Sr	1188	1158	1142
Zr	608	599	674
Nb	192	195	217
Ba	909	879	981
La	108	106	116
Ce	218	210	230
Sm	13.9	14.3	15.5
Eu	4.1	3.9	4.0
Tb	1.7	1.6	1.8
Yb	3.9	3.7	4.1
Lu	0.6	0.6	0.6

\* R<sup>2</sup> is the square of the residuals.

contains nepheline. Observed trace element concentrations in the Ne benmoreite are similar to those predicted by model 1. Trace element concentrations predicted by model 2 are generally too high.

Evolution from Ne benmoreite to anorthoclase phonolite gave three solutions (Table 7). The same phases were fractionated in each model, but those in model 3 had less evolved compositions than in the other models. The predicted trace elements in model 1 are similar to those measured in the anorthoclase phonolite, with the exceptions of Zr and Sr, which are too low, and Ba, which is too high. In model 2, calculated Rb, Ba, La, and Ce are higher than observed, whereas Sr is too low. These discrepancies suggest that the amount of feldspar fractionation in model 2 is too high. In model 3, predicted Zr is lower than observed and Sr, light REE, and Ba are high.

Based on the trace element data, model 1 is preferred in each of the three steps. Ne hawaiiite is therefore a 45% residual liquid of basanite, and in turn Ne benmoreite is a 78% residual liquid of Ne hawaiiite. Anorthoclase phonolite is a 66% residual liquid of Ne benmoreite and a 23.5% residual liquid of basanite (Fig. 9). Of note in the models are the importance of olivine, clinopyroxene, opaque oxide, and apatite fractionation in each step and the increasing importance of feldspar fractionation. Negative Eu anomalies due to feldspar fractionation were compensated for by Eu enrichment as a result of clinopyroxene and apatite fractionation. Models involving kaersutite fractionation were attempted but no reasonable solutions were reached. This is consistent with the observed lack of kaersutite phenocrysts.

#### COMPARISON OF THE EREBUS AND DVDP LINEAGES

Lavas from Hut Point Peninsula, Ross Island, and cores from Dry Valley Drilling Project (DVDP) drill holes 1–3 on Hut Point Peninsula have been investigated by Kyle & Treves

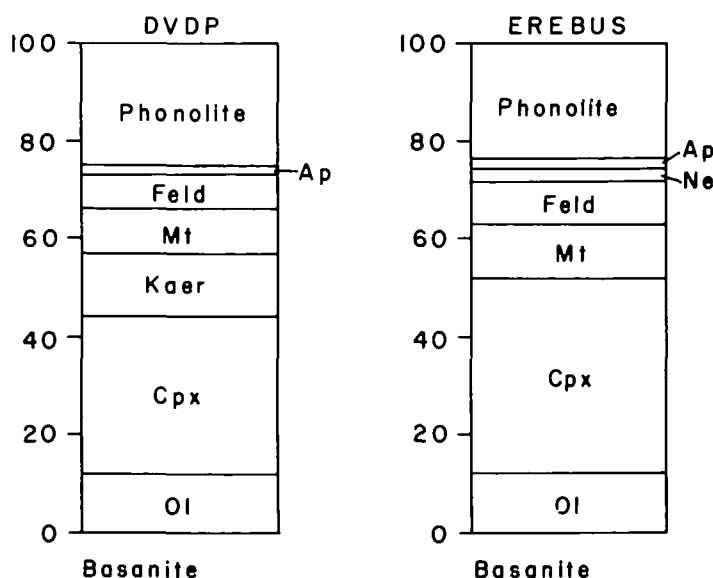


FIG. 9. Comparison of the relative proportions of mineral phases fractionated from a parental basanite to form phonolite in the Erebus and DVDP lineages. The vertical scale is in wt. % and shows the amount of phonolite residual liquid remaining and the amount of the mineral phase removed during fractionation. Ol—olivine, Cpx—clinopyroxene, Kaer—kaersutite, Mt—magnetite and spinel, Feld—feldspar, Ne—nepheline, Ap—apatite.

TABLE 7

Least-squares mass balance models for derivation of anorthoclase phonolite (83446) from *Ne benmoreite* (83410)

868

	Observed anorthoclase phonolite	Calculated anorthoclase phonolite		
		1	2	3
SiO <sub>2</sub>	51.49	51.50	51.49	51.48
TiO <sub>2</sub>	1.98	2.00	1.99	2.19
Al <sub>2</sub> O <sub>3</sub>	19.18	19.16	19.19	19.24
FeO*	7.89	7.89	7.88	7.81
MnO	0.23	0.22	0.21	0.24
MgO	2.23	2.22	2.24	2.31
CaO	5.63	5.61	5.63	5.56
Na <sub>2</sub> O	7.00	7.02	6.98	6.91
K <sub>2</sub> O	3.43	3.36	3.45	3.47
P <sub>2</sub> O <sub>5</sub>	0.94	0.96	0.94	1.03
Wt. fraction anorthoclase phonolite		0.6630	0.6112	0.7129
Olivine	(Fo <sub>38</sub> Ap)	0.0049	(Fo <sub>38</sub> Ap)	0.0062
Clinopyroxene	(En <sub>39</sub> Ap)	0.0718	(En <sub>39</sub> Ap)	0.0743
Ti magnetite	(Usp <sub>61</sub> Nh)	0.0550	(Usp <sub>61</sub> Nh)	0.0572
Feldspar	(An <sub>44</sub> Nm)	0.1262	(An <sub>33</sub> Nb)	0.1779
Nepheline	(Ne <sub>2</sub> )	0.0665	(Ne <sub>1</sub> )	0.0589
Apatite		0.0156		0.0157
Sum		1.0029	1.0015	0.0048
Sum R <sup>2*</sup>		0.01	0.00	0.08
<i>Trace element abundances (ppm) in anorthoclase phonolite</i>				
	<i>Observed</i>		<i>Calculated</i>	
Rb	106	110	119	103
Sr	885	767	592	1106
Zr	927	839	897	828
Nb	255	237	252	250
Ba	930	1090	1062	1223
La	109	113	136	126
Ce	219	223	233	245
Sm	13.3	12.5	13.1	14.1
Eu	4.2	3.6	3.6	4.0
Tb	1.7	1.5	1.9	1.8
Yb	4.9	4.3	4.6	4.5
Lu	0.8	0.7	0.7	0.8

P. R. KYLE ET AL.

(1974), Goldich *et al.* (1975, 1981), Sun & Hanson (1975, 1976), Kyle & Rankin (1976), Kyle (1981a, 1981b), and Stuckless *et al.* (1981). The Hut Point Peninsula and DVDP lavas form a lineage consisting of basanite, Ne hawaiiite, Ne mugearite, Ne benmoreite, and phonolite, termed the DVDP lineage (Kyle, 1981b). These lavas typically have kaersutite as phenocrysts or in the groundmass. Kaersutite is lacking in EL lavas.

Major and trace element trends of the EL and DVDP lineage can be compared in Figs. 6 and 7. Extrapolations of the trends are consistent with a similar parental magma for both lineages. At evolved compositions, the EL has lower concentrations of  $\text{Al}_2\text{O}_3$  and  $\text{Na}_2\text{O}$ , as a result of greater fractionation of nepheline and feldspar compared with the DVDP lineage.  $\text{TiO}_2$  and  $\text{FeO}^*$  are slightly lower in most evolved rocks of the DVDP lineage, consistent with kaersutite fractionation.  $\text{P}_2\text{O}_5$  shows a moderate decline in the EL, but drops off dramatically between evolved basanite and Ne hawaiiite in the DVDP lineage. This suggests a larger amount of apatite fractionation earlier in the evolution of the DVDP lineage. Watson (1979) showed that apatite saturation decreases markedly with decreasing temperature. The decline in  $\text{P}_2\text{O}_5$  may be the result of a significant change in temperature between the evolution from basanite and Ne hawaiiite in the DVDP lineage but not in the EL. This is possibly due to the EL evolving in a larger, deeper, and hotter magma chamber.

For the compatible trace elements Cr, Ni, and Cu the two lineages show similar sharp declines in concentrations as a result of combined fractionation of olivine, clinopyroxene, kaersutite, and Fe–Ti oxides. Intermediate and evolved rocks of the EL are depleted in V (Fig. 7) relative to DVDP rocks, consistent with the greater amount of Fe–Ti oxide fractionation in the EL than in the DVDP lineage.

Rb is more enriched in DVDP lineage lavas (Fig. 7). This can be attributed to the fractionation of anorthoclase from the EL. The Erebus and DVDP lineages show different K/Rb trends. The most basic rocks of both lineages have similar K/Rb ratios, but the ratio decreases with increasing differentiation in the DVDP lineage whereas it remains essentially constant in the EL. Kaersutite has a high K/Rb; thus, this ratio may be the best indicator of kaersutite fractionation (Kyle, 1981b).

Sr increases in the Erebus and DVDP lineages from basanite to Ne hawaiiite, then decreases systematically from Ne hawaiiite to phonolite, reflecting apatite and feldspar fractionation in the intermediate and evolved magmas of both lineages. However, Sr decreases more sharply in the EL than the DVDP lineage, consistent with its greater degree of feldspar and apatite fractionation. Although the basic rocks of the Erebus and DVDP lineages have similar Y concentrations, Y increases in the Erebus lineage with increasing differentiation but declines in the DVDP lineage, consistent with kaersutite fractionation.

Ba shows a trend of continuing enrichment with differentiation in the EL, whereas in the DVDP lineage Ba increases in basic rocks and stays approximately constant with increasing differentiation in intermediate and evolved rocks. This implies a bulk distribution coefficient of  $\sim 1.0$  for Ba during fractionation of the DVDP lineage, probably as a result of removal of kaersutite and anorthoclase (Goldich *et al.*, 1981; Kyle, 1981b). Zr, Hf, and Th increase uniformly in both the Erebus and DVDP suites, consistent with their high incompatibility.

Kyle (1981b) used least-squares mass balance calculations to model the evolution of the DVDP lineage by fractional crystallization from basanite to phonolite in steps similar to the three steps used to model the EL. Kaersutite fractionation was important in each step of the DVDP models. The total amount of crystallization of the basanite parental magma necessary to produce phonolite was similar in the EL (76.5%) and the DVDP lineage (74.9%) (Fig. 9). However, in the EL models the total cumulates contain no kaersutite, and proportionately greater amounts of olivine, apatite, clinopyroxene, Fe–Ti oxides, and

feldspar compared with the DVDP lineage model. Also, nepheline is fractionated in the evolution from Ne benmoreite to anorthoclase phonolite in the EL model. The fractionation of kaersutite in the DVDP lineage suggests that the magmas were more hydrous and probably lower in temperature than the EL magmas.

### PETROGENESIS OF EFS LAVAS

Enriched iron series (EFS) benmoreite, phonolite, and trachyte are volumetrically insignificant on Mt. Erebus. They show a distinctive trend on an AFM plot, an FeO\* vs. SiO<sub>2</sub> plot (Fig. 6), and on incompatible element plots (e.g., Fig. 7, Rb). These trends suggest that EFS lavas are not related to the EL by crystal fractionation but may have evolved from a geochemically distinct parental magma or by a separate fractionation process from a primitive basanite similar to that for the EL.

Trachyte from Aurora Cliffs has an <sup>87</sup>Sr/<sup>86</sup>Sr value of 0.70425, significantly higher than that of any EL lava. Another trachyte from Mt. Cis has an elevated <sup>207</sup>Pb/<sup>204</sup>Pb ratio (Sun & Hanson, 1976) compared with other Erebus volcanic province rocks, and the <sup>87</sup>Sr/<sup>86</sup>Sr value is similar to that for the Aurora Cliffs trachyte (Stuckless & Ericksen, 1976). Crustal xenoliths are common at Mt. Cis, and we interpret the high isotopic ratios in the trachytes as the result of crustal contamination. The high incompatible element concentrations, low concentrations of Sr and Ba, low K/Rb ratios, and large negative Eu anomalies of all the trachytes also suggest that they represent residual liquids from extreme fractionation, especially of alkali feldspar. The trachytes probably evolved by an assimilation–fractional crystallization process, possibly from the EFS benmoreites.

### EREBUS PLUME

It is apparent that Mt. Erebus represents a site of significant basanite magma production, which differentiates to anorthoclase phonolite. To account for the large volumes of magma erupted at Mt. Erebus it is necessary to invoke the presence of a mantle plume (the Erebus plume) to underlie the volcano.

Using simplified arguments and calculations, we can calculate the apparent rise rate of the plume. Dibble *et al.* (1984) have estimated the volume of Mt. Erebus to be 1700 km<sup>3</sup>. Surface exposures on Mt. Erebus are almost exclusively anorthoclase phonolite, with minor intermediate compositions at Fang Ridge and in the Dellbridge Island and vicinity. At present, all evidence suggests that the volcano is composed predominantly of anorthoclase phonolite. If we assume the volume is 50% phonolite, then we have ~850 km<sup>3</sup> of phonolite. Coastal exposures show that the phonolites occur mainly as thick dense flows. There is very little evidence of significant pyroclastic deposits. This is supported by measured seismic velocities of >4 km/s within the mountain (Dibble *et al.*, 1988). Allowing for 20% void space because of vesiculation and pyroclastic rocks gives a phonolite volume of 680 km<sup>3</sup>. As our models have shown, the phonolite represents a 25% residual liquid from a mantle-derived basanite parental magma. Therefore the volume of basanite necessary to generate the phonolites is 2720 km<sup>3</sup>.

We have assumed that Mt. Erebus is composed of 50% phonolite. The remaining 50% is probably Ne hawaiiite to Ne benmoreite, with minor basanite. If we assume these 850 km<sup>3</sup> also have 20% void space, this gives a volume of 680 km<sup>3</sup>. Our model (Table 5) shows that the Ne hawaiiite is a 45% residual liquid from the same basanite parent as the anorthoclase phonolite. Assuming this remaining 680 km<sup>3</sup> averages out to be an ~50% residual liquid,

then this requires another  $1360 \text{ km}^3$  of basanite. Therefore the total volume of basanite necessary to account for Mt. Erebus is  $4080 \text{ km}^3$ .

Basanite forms as a low-degree partial melt of garnet lherzolite mantle (Green, 1970). REE data suggest that typical McMurdo Volcanic Group basanite forms by  $<2\%$  partial melting of mantle peridotite (Kay & Gast, 1973; Kyle & Rankin, 1976). If we use  $5\%$  as a conservative estimate of the degree of partial melting, then the volume of mantle required to generate the rocks exposed on Mt. Erebus is  $82000 \text{ km}^3$ . This assumes that each batch of basanite must be derived from a new volume of mantle material. We believe this is reasonable, in view of the depleted nature of the mantle as indicated by the low  $^{87}\text{Sr}/^{86}\text{Sr}$  value of 0.703 and the high incompatible element concentrations in the basanites. One episode of partial melting would deplete the inventory of incompatible elements.

The volume of mantle required to generate the rocks is therefore extremely large. The mantle would rise as a plume and undergo partial melting in the garnet stability field (Fig. 10). If we assume this plume is the diameter of Mt. Erebus,  $\sim 40 \text{ km}$ , then a cylinder  $65 \text{ km}$  long would be needed. The oldest rocks on Mt. Erebus are dated at  $1 \text{ Ma}$ ; therefore the rise rate of the Erebus plume would be about  $65 \text{ mm/yr}$ .

Details of the above calculations are not important; however, there is no escaping the fact that large volumes of mantle are required to account for the voluminous anorthoclase phonolites. This, by necessity, requires significant mantle upwelling, presumably in the form of a plume, to account for the formation of Mt. Erebus.

The volcanic centers of Mt. Bird, Mt. Terror, and Hut Point Peninsula on Ross Island are radial about Mt. Erebus at  $\sim 120^\circ$  (Fig. 10). Large volumes of basanite would be generated

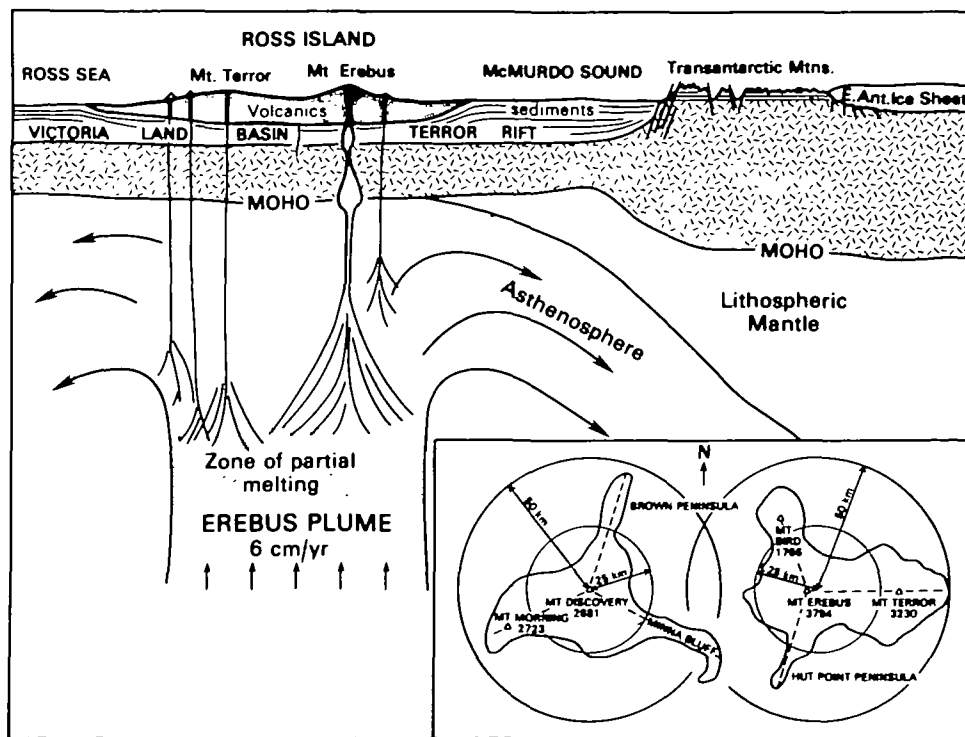


FIG. 10. Model of the Erebus mantle plume (not to scale). Inserts show the radial distribution of volcanic vents about Mt. Erebus and Mt. Discovery.

under Mt. Erebus to account for the large volumes of phonolite, whereas the extent of magma generation would be lower at the three surrounding volcanic centers, which are mainly basanite and Ne hawaiite. Phonolites occur but are uncommon and form only small cones.

The difference in the rate of magma generation could be due to lower temperatures in the outer part of the plume, resulting from interaction with surrounding cooler mantle, or the rise rate of the plume may be significantly faster at the center. In addition, differentiation of the basanite at Mt. Erebus occurred under hotter and drier conditions, giving rise to the Erebus lava lineage. At the three surrounding centers, the lavas belong to the DVDP lineage and fractionated with higher  $P_{\text{H}_2\text{O}}$  and at lower temperatures, presumably in smaller and higher-level magma chambers.

A radial distribution of vents similar to those on Ross Island is seen in southern McMurdo Sound, where Mt. Discovery (Fig. 10) is radially surrounded at 120° angles by Minna Bluff, Brown Peninsula, and Mt. Morning. It is possible that these centers are an early manifestation of the Erebus plume. Volcanic centers on Ross Island are dated at < 4 Ma, whereas in the Mt. Discovery area volcanism extends back to 19 Ma (Kyle & Muncy, 1989). Mt. Discovery is ~5 Ma old and is composed of highly evolved lavas, similar to Mt. Erebus (Kyle, 1976; Wright-Grassham, 1987). Assuming the mantle plume is fixed, it is therefore necessary to invoke a southward movement of the Antarctic plate between 4 and 5 Ma ago.

The Transantarctic Mountains (Fig. 10) to the west of Mt. Discovery form the imposing Royal Society Range with elevations exceeding 4 km. Uplift in the area is amongst the greatest in the Transantarctic Mountains. It is possible that the Erebus plume, during its early development and before the initiation of significant volcanism, enhanced the already occurring uplift (Fitzgerald *et al.*, 1986) of the mountain range.

Ross Island lies at the southern end of the Terror Rift, a major graben structure in the western Ross Sea (Cooper *et al.*, 1987). Extension within the rift probably started in mid-Tertiary time. It is possible that initiation and development of the Terror Rift and the Erebus plume coincided. Crustal extension could be a consequence of the plume.

## CONCLUSIONS

Phonolites in the Erebus and DVDP lineages represent a similar amount (~24%) of residual liquid derived by fractional crystallization from a basanite parental magma. However, the EL anorthoclase phonolite evolved at a higher temperature and lower  $P_{\text{H}_2\text{O}}$  than the DVDP lineage phonolite. In comparison, the DVDP lineage shows evidence of having evolved in small, individual magma chambers at lower temperatures (Kyle, 1981b).

The different mineralogy and geochemistry of the EFS suggest that it evolved from a different parental magma from that of the EL, possibly alkali basalt formed by higher degrees of partial melting in the mantle. The trachytes have elevated Pb and Sr isotopic ratios, suggesting evolution by assimilation fractional crystallization.

The threefold radial configuration of volcanic centers at Ross Island may be the result of radial crustal fractures above a small mantle plume centered beneath Mt. Erebus (Kyle & Cole, 1974; Kyle, 1987). Low degrees of partial melting in this plume formed the basanite parental magmas of the Erebus and DVDP lineages. EL lavas evolved in magma chambers fed by the main part of the plume, whereas basanites at the edges of the plume were at lower temperatures and pressures and crystallized kaersutite, forming the DVDP lineage rocks.

## ACKNOWLEDGEMENTS

We thank ITT Antarctic Services, Division of Polar Programs, NSF, and the US Navy VXE-6 squadron for assistance in undertaking fieldwork. We also thank the many people, especially Bill McIntosh, for their help in the field. Neutron irradiations were performed at the Research Reactor Facility, University of Missouri, under the Department of Energy Reactor Sharing Program. K. Keil, University of New Mexico, kindly made access available to his microprobe facility. J. Gamble and M. Menzies are thanked for constructive reviews. Early drafts of the manuscript were completed while P. R. K. was on leave at Royal Holloway and Bedford New College, University of London. We appreciate the assistance of Jennifer Callard and Connie Apache in preparation of the manuscript, and of Gerry Ingram in the Isotope Laboratory. This work was mainly supported by grants from the Division of Polar Programs, NSF.

## REFERENCES

- Aoki, K., 1964. Clinopyroxenes from alkaline rocks of Japan. *Am. Miner.* **49**, 119–23.
- 1968. Petrogenesis of ultrabasic and basic inclusion in alkali basalts, Iki Island, Japan. *Ibid.* **53**, 241–56.
- Armstrong, R. L., 1978. K–Ar dating: Late Cenozoic McMurdo Volcanic Group and Dry Valley glacial history, Victoria Land, Antarctica. *N.Z.J. Geol. Geophys.* **21**, 685–98.
- Arth, J. G., 1976. Behavior of trace elements during magmatic processes—a summary of theoretical models and their applications. *J. Res. U.S. Geol. Surv.* **4**, 41–7.
- Bence, A. E., & Albee, A. L., 1968. Empirical correction factors for the electron microanalysis of silicates and oxides. *J. Geol.* **76**, 382–402.
- Bryan, W. B., Finger, L. W., & Chayes, F., 1969. Estimating proportions in petrographic mixing equations by least-squares approximation. *Science* **163**, 926–7.
- Coombs, D. S., & Wilkinson, J. F. G., 1969. Lineages and fractionation trends in undersaturated volcanic rocks from the East Otago Volcanic Province (New Zealand) and related rocks. *J. Petrology* **10**, 440–501.
- Cooper, A. K., Davey, F. J., & Behrendt, J. C., 1987. Seismic stratigraphy and structure of the Victoria Land basin, western Ross Sea, Antarctica. In: Cooper, A. K., & Davey, F. J. (eds.) *The Antarctic Continental Margin: Geology and Geophysics of the Western Ross Sea*. Houston, TX: Earth Science Series of the Circum-Pacific Council for Energy and Resources, 27–65.
- Deer, W. A., Howie, R. A., & Zussman, J., 1966. *An Introduction to the Rock-Forming Minerals*. London: Longmans, 528 pp.
- Dibble, R. R., Barrett, S. I. D., Kaminuma, K., Miura, S., Kienle, J., Rowe, C. A., Kyle, P. R., & McIntosh, W. C., 1988. Time comparisons between video and seismic signals from explosions in the lava lake of Erebus volcano, Antarctica. *Disaster Prevention Res. Inst. Bull., Kyoto Univ.* **38**(337), 49–63.
- Kienle, J., Kyle, P. R., & Shibuya, K., 1984. Geophysical studies of Erebus volcano, Antarctica, from 1974 December to 1982 January. *N.Z. J. Geol. Geophys.* **27**, 425–55.
- Fitzgerald, P. G., Sandiford, M., Barrett, P. J., & Gleadow, A. J. W., 1986. Asymmetric extension associated with uplift and subsidence in the Transantarctic Mountains and Ross Embayment. *Earth Planet. Sci. Lett.* **81**, 67–78.
- Gibb, F. G. F., 1973. The zoned clinopyroxenes of the Shiant Isles sill, Scotland. *J. Petrology* **14**, 203–30.
- Goldich, S. S., Stuckless, J. S., Suhr, N. H., Bodkin, J. B., & Wamser, R. C., 1981. Some trace element relationships on the Cenozoic volcanic rocks from Ross Island and vicinity. In: McGinnis, L. D. (ed.) *Dry Valley Drilling Project. Antarctic Research Series, Vol. 33*. Washington, DC: Am. Geophys. Union, 215–28.
- Treves, S. B., Suhr, H. H., & Stuckless, J. S., 1975. Geochemistry of the Cenozoic volcanic rocks of Ross Island and vicinity, Antarctica. *J. Geol.* **83**, 415–35.
- Green, D. H., 1970. The origin of basaltic and nephelinitic magmas. *Trans. Leicester Lit. Phil. Soc.* **64**, 28–54.
- Haggerty, S. E., 1976. Opaque mineral oxides in terrestrial igneous rocks. In: Rumble, D., III (ed.) *Oxide Minerals, Miner. Soc. Am. Short Course Notes 3*, Hg101–Hg300.
- Heming, R. F., & Carmichael, I. S. E., 1973. High temperature pumice flows from the Rabaul Caldera, Papua, New Guinea. *Contr. Miner. Petrol.* **38**, 1–20.
- Jacobs, J. W., Korotev, R. L., Blanchard, D. P., & Haskins, L. A., 1977. A well-tested procedure for instrumental neutron activation analysis of silicate rocks and minerals. *J. Radioanal. Nucl. Chem.* **40**, 98–114.
- Jones, L., Faure, G., Taylor, K. S., & Corbato, C. E., 1983. The origin of salts of Mount Erebus and along the coast of Ross Island, Antarctica. *Isotope Geosci.* **1**, 57–64.
- Kay, R., & Gast, P. W., 1973. The rare earth content and origin of alkali-rich basalts. *J. Geol.* **81**, 653–82.
- Kohler, T., & Brey, G., 1990. Calcium exchange between olivine and clinopyroxene calibrated as a geothermobarometer for natural peridotites from 2 to 60 kb with applications. *Geochim. Cosmochim. Acta* **54**, 2375–88.

- Kyle, P. R., 1976. Geology, mineralogy, and geochemistry of the Late Cenozoic McMurdo Volcanic Group, Victoria Land, Antarctica. Unpublished Ph.D. Thesis, Department of Geology, Victoria University of Wellington, 444 pp.
- 1977. Mineralogy and glass chemistry of recent volcanic ejecta from Mt. Erebus, Ross Island, Antarctica. *N.Z.J. Geol. Geophys.* **20**, 1123–46.
- 1981a. Geologic history of Hut Point Peninsula as inferred from DVDP 1, 2, and 3 drillcores and surface mapping. In: McGinnis, L. D. (ed.) *Dry Valley Drilling Project, Antarctic Research Series, Vol. 33*. Washington, DC: Am. Geophys. Union, 427–45.
- 1981b. Mineralogy and geochemistry of a basanite to phonolite sequence at Hut Point Peninsula, Antarctica, based on core from Dry Valley Drilling Project drillholes 1, 2, and 3. *J. Petrology* **22**, 451–500.
- 1986. Mineral chemistry of Late Cenozoic McMurdo Volcanic Group rocks from The Pleiades, northern Victoria Land. In: Stump, E. (ed.) *Geological Investigations in Northern Victoria Land. Antarctic Research Series, Vol. 41*. Washington, DC: Am. Geophys. Union, 305–37.
- 1987. The Erebus Hotspot; mantle upwelling in McMurdo Sound, Antarctica (Abstract). *Proc. 5th Int. Symp. Antarctic Earth Sci., Cambridge*, p. 85.
- 1990a. McMurdo Volcanic Group–Western Ross Embayment: introduction. In: LeMasurier, W., & Thompson, J. (eds.) *Volcanoes of the Antarctic Plate and Southern Oceans. Antarctic Research Series, Vol. 48*. Washington, DC: Am. Geophys. Union, 18–25.
- 1990b. Erebus Volcanic Province: summary. *Ibid.*, 81–8.
- Cole, J. W., 1974. Structural control of volcanism in the McMurdo Volcanic Group, Antarctica. *Bull. Volcanol.* **38**, 16–25.
- Dibble, R. R., Giggenbach, W. F., & Keys, J., 1982. Volcanic activity associated with the anorthoclase phonolite lava lake, Mt. Erebus, Antarctica. In: Craddock, C. (ed.) *Antarctic Geosciences*. Madison: University of Wisconsin Press, 735–45.
- Muncy, H. L., 1989. Geology and geochronology of McMurdo Volcanic Group rocks in the vicinity of Lake Morning, McMurdo Sound, Antarctica. *Antarctic Sci.* **1**, 345–50.
- Rankin, P. C., 1976. Rare earth element geochemistry of Late Cenozoic alkaline lavas of the McMurdo Volcanic Group, Antarctica. *Geochim. Cosmochim. Acta* **40**, 1497–507.
- Treves, S. B., 1974. Geology of Hut Point Peninsula, Ross Island. *Antarctic J. U.S.* **9**, 232–4.
- Le Bas, M. J., Le Maitre, R. W., Streckeisen, A., & Zanettin, B., 1986. A chemical classification of volcanic rocks based on the total alkali–silica diagram. *J. Petrology* **27**, 745–50.
- Le Roex, A. P., 1985. Geochemistry, mineralogy, and magmatic evolution of the basaltic and trachytic lavas from Gough Island, South Atlantic. *Ibid.* **26**, 149–86.
- Lindstrom, D. J., & Korotev, R. L., 1982. TEABAGS: computer programs for instrumental neutron activation analysis. *J. Radioanal. Nucl. Chem.* **70**, 439–58.
- Mason, R. A., Smith, J. V., Dawson, J. B., & Treves, S. B., 1982. A reconnaissance of trace elements in anorthoclase megacrysts. *Miner. Mag.* **46**, 7–11.
- Moore, J. A., & Kyle, P. R., 1987. Volcanic geology of Mt. Erebus, Ross Island, Antarctica. In: *Proc. NIPR Symp. Antarctic Geosci., No. 1*. Tokyo: National Institute of Polar Research, 48–65.
- Norrish, K., & Chappell, B. W., 1977. X-ray fluorescence spectrometry. In: Zussman, J. (ed.) *Physical Methods in Determinative Mineralogy*, 2nd Edn. New York: Academic Press, 201–72.
- Papike, J. J., Cameron, K. L., & Baldwin, K., 1974. Amphiboles and pyroxenes: characterization of other than quadrilateral components and estimates of ferric iron from microprobe data. *Geol. Soc. Am. Abstr. Prog.* **6**, 1053–4.
- Price, R. C., Johnson, R. W., Gray, C. M., & Frey, F. A., 1985. Geochemistry of phonolites and trachytes from the summit region of Mt. Kenya. *Contr. Miner. Petrol.* **89**, 394–409.
- Schnetzler, C. C., & Philpotts, J. A., 1970. Partition coefficients of rare earth elements between igneous matrix material and rock-forming mineral phenocrysts II. *Geochim. Cosmochim. Acta* **34**, 331–40.
- Stephenson, D., 1972. Alkali clinopyroxenes from nepheline syenites of the South Qoroq centre, South Greenland. *Lithos* **5**, 187–201.
- Stormer, J. C., Jr., 1983. The effects of recalculation on estimates of temperature and oxygen fugacity of multicomponent iron–titanium oxides. *Am. Miner.* **68**, 586–94.
- Stuckless, J. S., & Ericksen, R. L., 1976. Sr isotope geochemistry of the volcanic rocks and associated megacrysts and inclusions from Ross Island and vicinity, Antarctica. *Contr. Miner. Petrol.* **58**, 111–26.
- Miesch, A. T., Goldich, S. S., & Weiblen, P. W., 1981. A Q-mode factor for the petrogenesis of the volcanic rocks from Ross Island and vicinity, Antarctica. In: McGinnis, L.D. (ed.) *Dry Valley Drilling Project. Antarctic Research Series, Vol. 33*. Washington, DC: Am. Geophys. Union, 257–80.
- Sun, S. S., & Hanson, G. N., 1975. Origin of Ross Island basanitoids and limitations upon the heterogeneity of the mantle sources for alkali basalts and nephelinites. *Contr. Miner. Petrol.* **52**, 77–106.
- 1976. Rare earth evidence of differentiation of McMurdo Volcanics, Ross Island, Antarctica. *Ibid.* **54**, 139–55.
- Takahashi, E., 1978. Partitioning of  $\text{Ni}^{2+}$ ,  $\text{Fe}^{2+}$ ,  $\text{Mn}^{2+}$  and  $\text{Mg}^{2+}$  between olivine and silicate melts: compositional dependence of partition coefficients. *Geochim. Cosmochim. Acta* **42**, 1829–44.
- Taylor, S. R., & Gorton, M. P., 1977. Geochemical application of spark source mass spectrography—III. Element sensitivity, precision and accuracy. *Ibid.* **41**, 1375–80.

- Toulmin, P., III, & Barton, P. B., 1964. A thermodynamic study of pyrite and pyrrhotite. *Ibid.* **28**, 641–71.
- Tuttle, O. F., & Bowen, N. L., 1958. Origin of granite in the light of experimental studies in the system  $\text{NaAlSi}_3\text{O}_8\text{--H}_2\text{O}$ . *Mem. Geol. Soc. Am.* **74**, 153 pp.
- Watson, E. B., 1977. Partitioning of manganese between forsterite and silicate liquid. *Geochim. Cosmochim. Acta* **41**, 1363–74.
- 1979. Apatite saturation in basic and intermediate magmas. *Geophys. Res. Lett.* **6**, 937–40.
- Wilkinson, J. F. G., 1956. Clinopyroxenes of alkali olivine-basalt magma. *Am. Miner.* **42**, 724–43.
- Wright-Grassham, A. C., 1987. Volcanic geology, mineralogy and petrogenesis of the Discovery volcanic subprovince, southern Victoria Land, Antarctica. Ph.D. Dissertation, New Mexico Institute of Mining and Technology, Socorro, 466 pp.
- Zindler, A., & Hart, S., 1986. Chemical geodynamics. *Ann. Rev. Earth Planet. Sci.* **14**, 493–571.